

Article

Enhancing Signal Quality of Capacitive Displacement Measurements in Machine Tool Environments [†]

Sebastian Böhl ^{1,*} , Sascha Weikert ² and Konrad Wegener ¹

¹ Institute of Machine Tools and Manufacturing (IWF), ETH Zürich, Leonhardstrasse 21, 8092 Zurich, Switzerland

² Inspire AG, Technoparkstrasse 1, 8005 Zurich, Switzerland

* Correspondence: boehl@iwf.mavt.ethz.ch; Tel.: +41-44-633-92-65

[†] This paper is an extended version of our paper published in Böhl, S.; Weikert, S.; Wegener, K. Improving robustness of capacitive displacement measurements against electromagnetic disturbances in machine tool environments. In Proceedings of the 13th International Conference and Exhibition on Laser Metrology, Machine Tool, CMM & Robotic Performance—Lamdmap XIII, Sheffield, UK, 13–14 March 2019.

Received: 29 June 2019; Accepted: 13 August 2019; Published: 30 August 2019



Abstract: Capacitive displacement sensors are a valuable choice for high accuracy geometric spindle measurements. Although these sensors show the specified performance in electromagnetic friendly environments, the performance may degrade drastically in machine tool environments due to electromagnetic disturbances. An in-situ testing procedure based on a cap test setup is proposed, which enables a simplified error diagnosis and verification of sensor performance. The functionality of the device and the application to different practical cases are presented. The results of these tests suggest that a decisive part of disturbances may couple into the measurement system via electrical conduction at interfaces between the machine tool and measurement device parts. Disturbances originate in the power electronics of the machine tool and are passed on to the safety ground of the machine tool, which is connected to all structural components of the machine tool. The proposed counter measure targets a complete galvanic separation of the measurement system from machine tool parts. The effectiveness of this counter measure was verified in different tests on two different machine tools. It is shown that the application of the galvanic separation leads to a comparable sensor performance in machine tool environments as achieved by the manufacturer under calibration conditions.

Keywords: capacitive displacement measurement; electromagnetic disturbance; robustness; calibration

1. Introduction

Machine tool testing is an essential task to enable improvements of machine tools, either in the field of scientific research or in the industrial development process. Further, acceptance tests are carried out to clear a machine tool for shipment. Finally, specifications of machine tools and corresponding testing procedures need to be defined, in order to choose a suitable machine tool for a desired manufacturing process [1].

ISO 230 series defines procedures for testing the accuracy of machine tools, regarding thermal, vibrational and contouring behavior. The geometric testing of machine tools incorporates the determination of error motions and errors regarding location and orientation of linear and rotary axes. Machine tool spindles play a central role for accurate machining. The tool or workpiece spindle is directly neighboring the material removal process. Thus, spindle error motions have a significant impact on the quality of the workpiece surface.

1.1. Spindle Error Motion

A spindle has to fulfill two major tasks. First, the spindle shall rotate the workpiece or the tool in space along a specified orientation and location of a rotation axis. Second, the spindle is responsible for transmitting the energy necessary for material removal to the cutting zone [2]. In addition to the desired pure rotation of the spindle rotor around the desired axis of rotation, undesired superposed error motions are present [3]. The determination of these errors is the task of testing procedures for geometric accuracy of axes of rotation. ISO 230-7 [4] defines the error motions of axis of rotation, namely radial, axial and tilt error motion. The direction of each error motion is defined in accordance with the machine tool coordinate system. In the case of a vertical spindle C, this yields to the following five error motions: two radial error motions in X- and Y-direction, two tilt error motions around the X- and Y-axis and one axial error motion (Figure 1a).

The basic measurement setup for geometric testing of tool spindles in accordance with ISO 230-7 [4] is depicted in Figure 1b. On the tool side, a test mandrel with a specified and calibrated geometry is mounted in the spindle. On the workpiece side, five contactless displacement sensors are installed in a sensor fixture, which is mounted on the machine tool table. These sensors measure against the test mandrel surface and determine, based on the gathered data, the location and orientation of the test mandrel in the coordinate system of the sensor fixture.

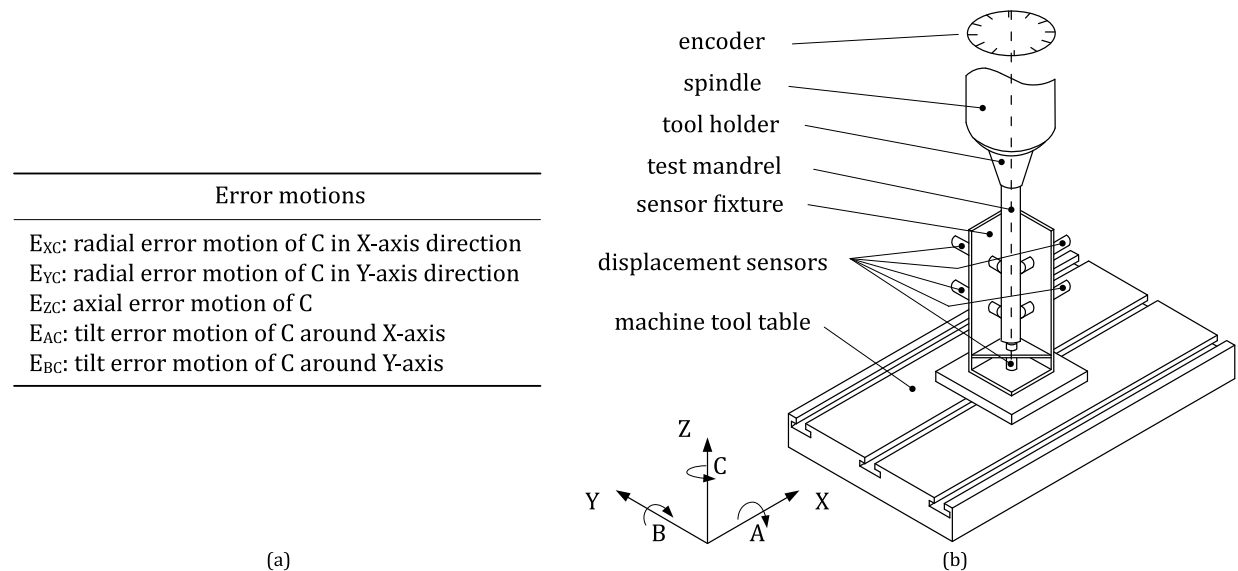


Figure 1. In accordance with ISO 230-7 [4]: (a) error motions of a vertical spindle C being nominally parallel to the vertical Z-axis; and (b) spindle measurement setup.

The increasing demand for higher geometric spindle accuracy requires a commensurate degree of measurement uncertainty, in order to enable the potential acceptance of specified error motion tolerances. The achievable accuracy is influenced by the design of the spindle. Especially, the type of bearing pre-determines the tolerances for error motions. Typical tolerances for three types of spindles are indicated in Table 1.

Table 1. Typical radial error motion tolerances for tool spindles depending on bearing type [5].

Spindle Type	Tolerance for Radial Error Motion E_{XC}			
air bearing spindle	1 nm	<	E_{XC}	≤ 100 nm
precision ball bearing	0.1 μm	<	E_{XC}	≤ 1 μm
standard machine tool spindle	1 μm	<	E_{XC}	

1.2. Capacitive Sensing in Spindle Metrology

Capacitive displacement sensors are a potential option as displacement sensors for spindle measurements. The underlying fundamental principle of this kind of displacement measurement is the determination of changes of capacitance between two electrodes due to changes in gap width [6]. In spindle measurements, the measuring electrode of the transducer and the test mandrel surface form the capacitor with variable gap width. An appropriate grounding of the test mandrel on the reference ground is essential. For this purpose, a grounding brush can be used [5]. Potential differences between grounded target surface and transducer need to be avoided [7].

A driver excites the measuring circuit with a specific carrier frequency and detects, filters and amplifies changes in the carrier signal. In a typical spindle measurement setup, sensor driver, sensor, evaluation circuit, and target are not encapsulated in one box. They are locally separated. This kind of configuration can be described as a distributed system [7]. Some parts of this distributed system are mechanically and electrically integrated into the machine tool environment. At the resulting interfaces, machine tool and measuring system interact. Thus, electromagnetic disturbances may couple into the measuring system and corrupt the measuring signal [5,7,8].

1.3. Electromagnetic Interference in Machine Tool Environments

The term electromagnetic interference (EMI) comprises the “degradation of the performance of an equipment, transmission channel or system caused by an electromagnetic disturbance” [9].

Three prerequisites are necessary for electromagnetic interference:

1. A disturbance source acting as disturbance sender is located at effective distance to the susceptible device.
2. To allow disturbances to travel from the sender to the receiver, links between both need to be established. Physical mechanisms such as electrical conduction and electromagnetic radiation potentially provide the mentioned coupling. Radiation as coupling mechanism may be further divided into mechanisms based on inductive and capacitive effects, which occur in the near field, whereas in the far field electromagnetic waves are significant [10].
3. The device has to be accessible for disturbances with respect to frequency range and disturbance power [11].

On the one hand, disturbance sources may be located within the measurement device and are thus an inherent characteristic of the measurement device itself. Depending on the circuit design of the evaluation electronics, different effects such as shot noise, excess noise in semiconductor junctions, and thermal noise in resistors may occur [8]. On the other hand, disturbance sources located in the environment of the measurement device are defined as external sources. Figure 2 shows a schematic categorization of disturbance source and sink interaction.

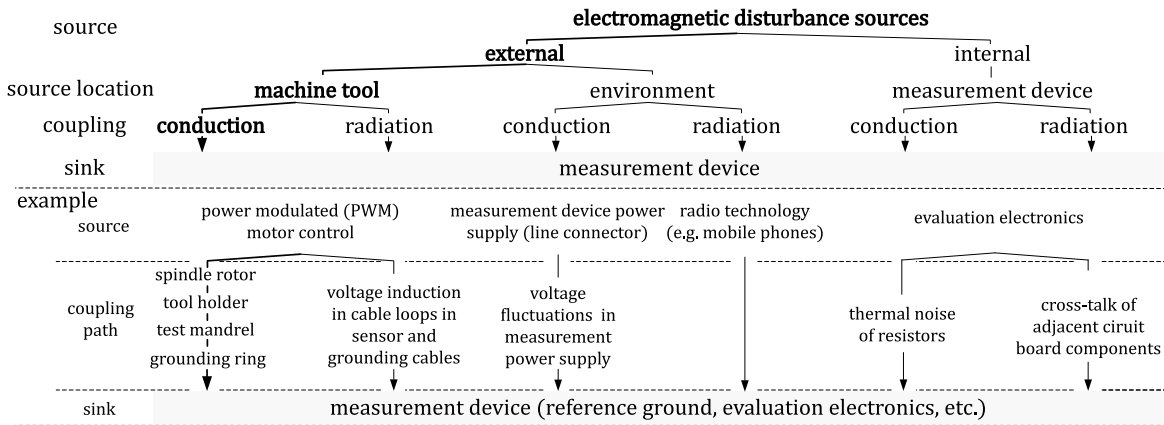


Figure 2. Categorization of electromagnetic interference mechanisms for capacitive displacement measurements in machine tool environments.

1.3.1. Disturbed Spindle Measurements in Machine Tool Environments

Figure 3 shows the schematic electrical arrangement of a spindle measurement. Capacitance changes of the impedance Z_M due to the displacement $u(t)$ of the spherical target are evaluated. The measuring impedance Z_M may be approximated as a combination of a measuring capacitance C_M , a loss resistance R_L and the resistance $R_{M,iso}$, representing the isolating behavior of the air gap [6].

The test mandrel is mechanically mounted in the spindle. Thus, it is electrically coupled to the spindle rotor via a contact impedance Z_{TM} , consisting of an ohmic resistance R_{iso} and a resulting capacity C_{iso} .

The grounding of the target on reference ground is accomplished via a grounding brush. The sliding contact between fibers and test mandrel surface is approximated by the impedance Z_{SGR} based on a time-varying ohmic resistance R_{SGR} and a capacity C_{SGR} .

Parasitic currents can occur in an inverter driven spindle unit. The inverter might generate steep voltage edges, which are propagated into a system of capacities between stator windings of the electrical motor, spindle rotor, spindle housing and bearings. This system is represented by impedances Z_{WH} , Z_{WR} , Z_{RH} , and Z_B (Figure 3). Currents are circulating in the loop of housing and spindle rotor, which are known as circular currents. In the case the rotor is connected to the reference ground, rotor shaft currents leak towards this ground [12].

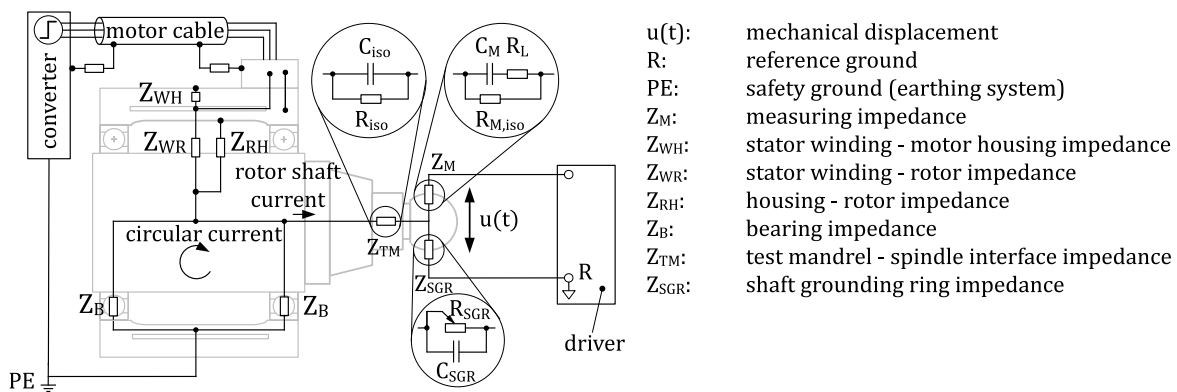


Figure 3. Schematic of interconnection between tool spindle and capacitive measurement device.

The interaction between measuring circuit and the machine tool circuit depends on the electrical properties of the interface between the test mandrel and the tool holder as well as the spindle rotor. Thus, the disturbances from the machine tool circuit may couple into the measurement system.

1.4. Potential Handling Strategies for Electromagnetically Disturbed Measurements

The disturbing influence of the machine tool on the capacitive displacement measurement can be reduced either by elimination of the disturbance source or by breaking the coupling path at the interfaces between machine tool and measurement device. If neither is possible, signal filtering approaches can be applied. In the following, the different methods are briefly discussed.

1.4.1. Temporary Elimination of Disturbance Sources

Sheridan [7] reported on the disturbing effects on spindle measurements induced by a DC motor in combination with a silicon controlled rectifier (SCR) type controller and pulse width modulation (PWM) type drives. The disturbances are visible as spikes in the measurement signal. Two recommendations for handling these effects in spindle measurements are given: First, an adaptation of the measurement procedure is proposed, which consists of a speed run up, then a drive power switch-off and finally measuring during run down. Second, in the process of signal analysis and after identifying the origin of the peak as being electrical and not mechanical based, the spikes in question are simply ignored.

The proposed methods are applicable, but have their shortcomings regarding the definition of the testing condition, flexibility of testing routines and repeatability or reproducibility of measurements. Further, the disturbance effects might not only result in a spiky signal, but also may result in distorted and noisy signals. Thus, excluding distorted parts of the signal is not easily possible any more.

1.4.2. Signal Filtering

Low-pass and notch filtering approaches seem promising in the case the error motion frequencies of interest are distinct from disturbance frequencies, in order to cut off or cut out spectral power of disturbance effects. The following example illustrates the limitations of this approach.

A high-frequency ball bearing spindle with a maximum speed of 40,000 rpm shall be tested. The current controller clock cycle is 500 μ s and the pulse frequency is 2 kHz with corresponding harmonics. The angular contact bearings consist of 16 balls. It has a pitch-circle diameter of 48.5 mm, a ball diameter of 7.9 mm, and a contact angle of 15°. Damages may potentially occur on the outer and inner ring, the balls as well as on the cage. Estimations for corresponding frequencies are given by Dresig [13]. The roundness deviation of the target is calibrated applying a roundness filter up to 15 undulations per revolution (UPR). In summary, frequency components of three sources contribute to the signal content. The influence of the pulse frequency of the pulse width modulated drive system is a machine tool disturbance, whereas the target roundness deviation is a disturbing influence of the test mandrel. The objective of the measurement is the detection of damages in the bearing system. Hence, the roundness deviation of the test mandrel needs to be corrected and power electronic effects shall be filtered.

The displacement sensor is assumed to have a low-pass characteristic (Figure 4a). The resulting frequencies due to the three introduced sources in dependency of the spindle speed n are depicted in Figure 4b. At Point P and speed n_{crit} , the pulse frequency line and the 15th UPR-line cross each other. Thus, the application of either a notch filter at pulse frequency and associated harmonics or a low-pass filter with cut-off frequency below the pulse frequency is only possible for rotational speeds reasonably below n_{crit} . Otherwise, signal contents associated with the bearing system and the test mandrel are erroneously attenuated. Thus, test programs are constrained by a maximum permissible spindle speed.

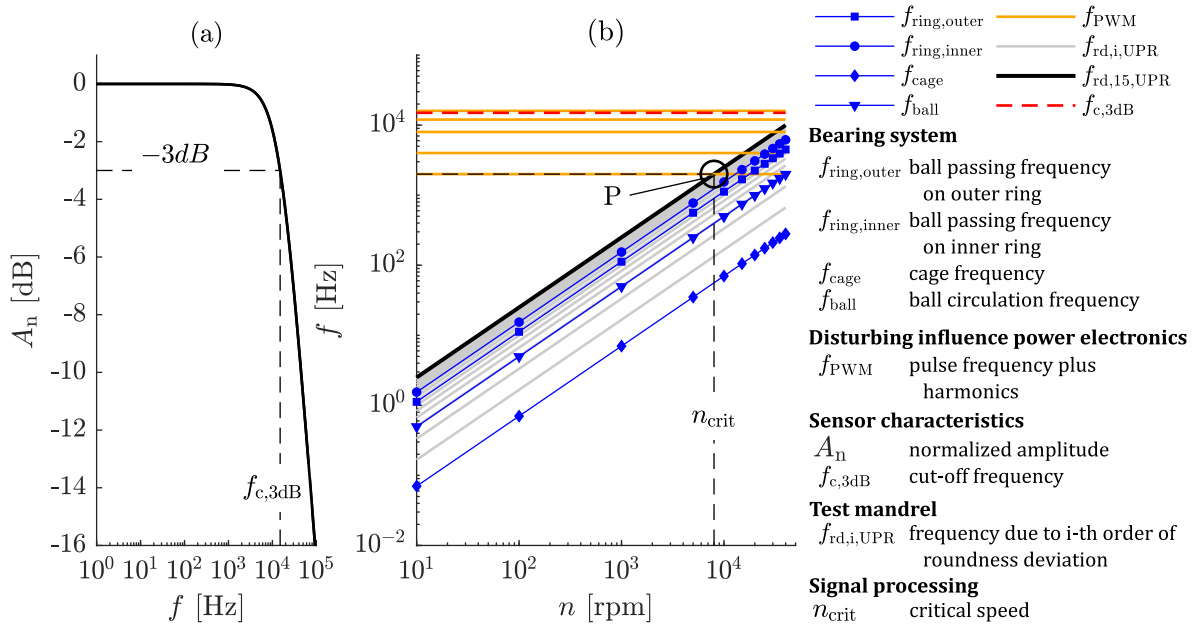


Figure 4. (a) Approximated frequency response of capacitive sensor; and (b) exemplary frequencies occurring in spindle measurements due to influences of power electronics, ball bearings, and target form deviation.

1.4.3. Disturbance Attenuation

The electromagnetic disturbance attenuation approach proposed in this work and according to [14] is based on a galvanic separation of the measurement setup from the machine tool. The principle behind this idea is exemplarily discussed in the following.

The interface between spindle and target is approximated by the impedance Z_{TM} (Figure 3). The implementation of appropriate electrical isolating elements at the interface hinders electrical conduction. Additionally, the resulting capacitive coupling needs to be attenuated.

In Figure 5a, a simplified equivalent circuit is illustrated. A full capacity bridge [15] is used as primary evaluation circuit with measuring capacity $C_M := C_1$. The circuit is driven by an alternating voltage U_s . The output voltage U_a is further processed in additional downstream electronics. The measuring circuit is integrated into a second circuit, which is driven by a disturbing voltage U_d . The isolation capacity C_{iso} represents the capacity of the isolating element between spindle and test mandrel. In this circuit configuration, the disturbance voltage is superposed to the measuring excitation voltage and has direct impact on the output voltage U_a .

The attenuation of the capacitive coupling demands the choice of the isolator such that, ideally, no voltage drop at the bridge occurs. The circuit depicted in Figure 5b is the equivalent circuit of the discussed disturbed measuring circuit, but taking only the disturbance source into account. The measuring bridge can be reduced to one capacity $C_{M,b}$, which is in series with the isolator capacity C_{iso} . The voltage, which drops at $C_{M,b}$, is regarded as the output of the disturbance source circuit, driven by the disturbing voltage U_d . Hence, the transfer function from disturbance source to measuring circuit is

$$G = \frac{U_{M,b}}{U_d} = \frac{\left(\frac{C_{iso}}{C_{M,b}}\right)}{\left(\frac{C_{iso}}{C_{M,b}}\right) + 1}. \tag{1}$$

The influence of the disturbance voltage source on the measuring circuit is in this case dependent on the ratio of the isolating capacity and the bridge capacity. Disturbances are attenuated for cases in which $(C_{M,b}/C_{iso}) \gg 1$ holds (Figure 5c). If the isolating capacity is chosen to be larger than the equivalent bridge capacity, the measuring circuit is disturbed significantly.

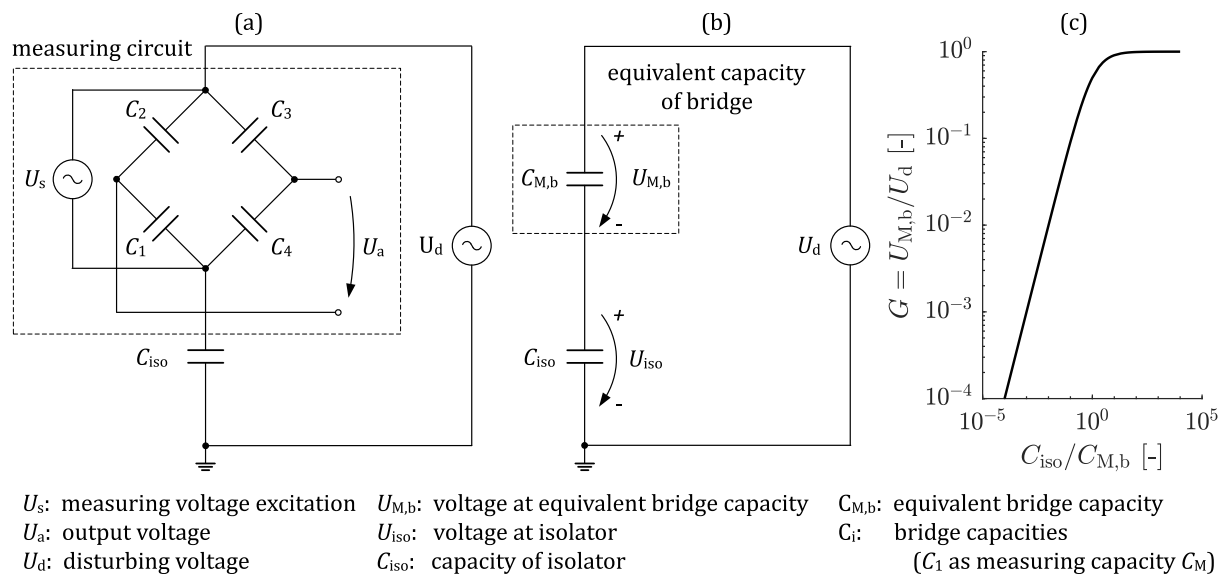


Figure 5. Schematic representation of a capacitive measuring circuit, interconnected to the electrical system of a machine tool: (a) capacitive displacement setup with primary evaluation based on a capacitive bridge; (b) equivalent circuit with condensed bridge capacity $C_{M,b}$; and (c) transfer function G in dependence of capacity ratio $C_{iso}/C_{M,b}$.

1.5. Objective of this Work

Electric power converters and controls are assumed to have a major disturbing impact on capacitive displacement measurement devices in machine tool environments [7]. Electromagnetic radiation is typically suspected as the responsible disturbance coupling mechanism.

However, electrical conduction is typically not considered. In this paper, the impact of electrical conduction as transmitting mechanism for disturbances is analyzed. This coupling mechanism plays an important role for spindle metrology. Typically, sensor fixtures, tool holder and test mandrels are made of uncoated steel. This also holds usually for the spindle rotor and the machine tool table. Hence, the installation of the measurement setup yields metallic bright interfaces between machine tool components and measurement setup components. These promote conduction as coupling mechanism. In contrast, a galvanic separation is assumed to attenuate the disturbance influence.

2. Materials and Methods

In the following sections, the spindle measurement device under test and the machine tool environments are specified. Subsequently, the novel testing device is discussed and the developed testing procedure is presented.

2.1. Measurement Device under Test

The capacitive measurement device for geometric spindle measurements used in this work is a Spindle Error Analyzer (SEA) made by LION PRECISION. The device has five displacement measurement channels, each constituted by a capacitive sensor ($C7-C$) and a corresponding driver (DMT20). The sensor was

operated in single-ended mode and the cylindrical sensor housing was directly connected to the reference ground of the device. Table 2 indicates further technical specifications and calibration data. The analog signal was digitized with a NATIONAL INSTRUMENTS™ analog-to-digital converter (NI USB-6251) with 16 bit resolution.

The test mandrel grounding was accomplished via a shaft grounding ring (AEGIS SGR®). The recommended silver paint was applied to the test mandrel to support conduction of the interface.

Table 2. Technical and calibration data of capacitive displacement measurement device.

Parameter	Unit	Channel				
		1	2	3	4	5
peak-to-peak value (<i>pp</i>)	[nm]	58.9	49.7	52.9	75.3	40.3
root-mean-square value (<i>y_{rms}</i>)	[nm]	6.6	5.2	5.5	6.1	5.0
Specifications:	output voltage	±10 V	sensitivity		80 mV/μm	
	measuring range	250 μm	near gap		125 μm	
	bandwidth	15 kHz				

2.2. Machine Tool Environments

Experiments were carried out in the laboratory of the Institute of Machine Tools and Manufacturing (IWF) on two different machine tools:

- Machine tool FEHLMANN Picomax® Versa 825 equipped with a HEIDENHAIN iTNC 530 control and a main computer MC 422C.
- Machine tool Präzoplan®, which is equipped with a SIEMENS SINUMERIK 840D SL CNC. Linear drives and the spindle are controlled by SINAMICS S120 modules.

The machine tools are indicated as Machine Tool A and Machine Tool B in the following discussion.

Although both machines differ in nominal power of the drive and spindle system, this class of machine is typically measured with the spindle measurement device described above. The power electronics and controls disturb the measurement device differently. Thus, the performance of the attenuation method can be tested in two contrary environments.

2.3. Determination of Sensor Behavior under Disturbance Influence

In general, a sufficient clearance between distortion and desired signal is necessary for a reliable extraction of the desired information content. To estimate this clearance, the signal-to-noise ratio (SNR) and the signal-to-interference ratio including noise and distortion (SINAD) are commonly used [16]. These measures set the signal power in relation to the power of noise and distortion. The effective number of bits (ENOB) gives an indication about the resolution of distorted signals gathered by analogous sensors, which are digitized using an analog-to-digital converter [17].

The input–output behavior of an unknown displacement sensor can be determined via dynamic calibration procedures. Breitenbach [16] analyzed the response of an analog sensor to a mechanical displacement excitation. Harmonic excitations with known amplitudes and frequencies are used in this calibration procedure. The transfer function from the input, with input signal $u(t)$ as well as disturbance input $v(t)$, to the output $y(t)$ characterizes the sensor process (Figure 6a,b—top row). In the output, disturbances are superposed to the signal. The performance indicator determined with these kinds of dynamic calibration procedures is the SNR.

A method to determine the inherent characteristics of a sensor and its behavior under disturbance influence is the so-called cap test [5,18]. A jig holds the sensor as well as the target rigidly, which results

in a tiny structural loop (Figure 6a,b—bottom row). Thus, the mechanical displacement input due to a relative target motion is suppressed. Therefore, the signal output of the capped sensor contains mainly effects due to external disturbances and the inherent sensor noise characteristics.

An adapted design of the cap test enables the analysis of different environmental influences. ISO 230-3 A.5 [18] describes a typical cap test setup for temperature stability tests. For an individual thermal disturbance response characterization of displacement sensors, a jig made of a material with low or almost zero thermal expansion coefficient can be used [19]. The jig design, which is presented in the following sections, targets the electromagnetic interference behavior.

In a cap test, the signal input is nominally set to zero, which means that the SNR equals zero. Thus, the performance measurand based on testing capped sensors is the signal power due to noise and distortion.

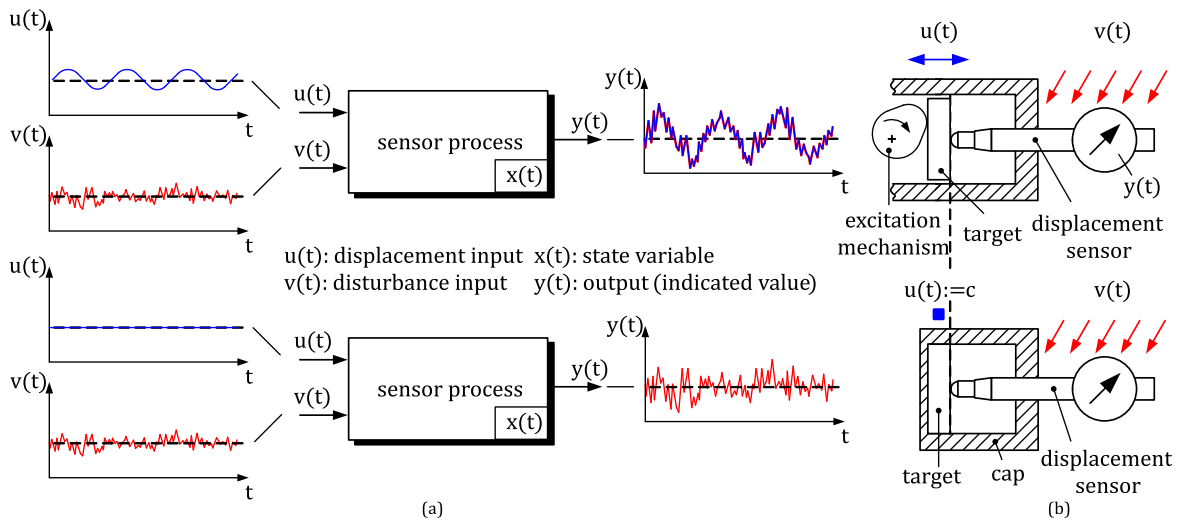


Figure 6. Determination of displacement sensor behavior with respect to mechanical displacement and disturbance input (**top**: mechanical harmonic excitation; **bottom**: capped sensor): (a) schematic signal diagram representation; and (b) realization of calibration procedure.

2.4. Assessment of Signal Quality

The measurement chain has an inherent noise behavior with a characteristic noise power. Environmental disturbances superpose this inherent noise characteristic. Since this noise power dictates the lower limit of detectable signal amplitudes, the resulting requirement is to limit the total noise power of the measurement device under harmful environmental conditions to the measurement device inherent noise power. The term signal quality is here defined as the degree of fulfilment of this requirement.

The signal power P_y of a continuous signal $y(t)$ in the time duration T can be calculated either in frequency or in time domain [20]. Its unit is the square of the physical unit of the signal, e.g., $[y(t)] = m$ and $[P_y] = m^2$. Hence, signal power cannot be interpreted in terms of physical power (unit watt).

Given the spectrum $Y(f)$ of a signal in frequency domain, the power of the signal is either determined directly by using the spectrum $Y(f)$ or the auto-power spectral density $S_{yy}(f)$,

$$P_y = \frac{1}{T} \int_{-\infty}^{\infty} |Y(f)|^2 df = \int_{-\infty}^{\infty} S_{yy}(f) df. \tag{2}$$

Parseval’s identity [20], which states that the energy of a signal is independent of the domain of representation, relates time and frequency domain,

$$\int_{-\infty}^{\infty} y^2(t) dt = \int_{-\infty}^{\infty} |Y(f)|^2 df. \tag{3}$$

The power of the signal $y(t)$ in time domain is defined as

$$P_y = \frac{1}{T} \int_0^T y^2(t) dt = \overline{y^2}. \tag{4}$$

Hence, the power P_y is equal to the square of the root-mean-square value y_{rms} ($:= \sqrt{\overline{y^2}}$). The characteristics of the signal $y(t)$ can additionally be characterized in terms of a statistical description in the amplitude domain via probability density functions (PDF) or cumulative distribution functions (CDF) [21]. The distribution function is described by statistical moments, which are closely related to the mean value, the variance, the skewness and the kurtosis. The root-mean-square value y_{rms} , the mean value \bar{y} ,

$$\bar{y} = \frac{1}{T} \int_0^T y(t) dt, \tag{5}$$

and the standard deviation σ_y ,

$$\sigma_y = \frac{1}{T} \int_0^T (y(t) - \bar{y})^2 dt, \tag{6}$$

are related among each other, according to the displacement law for variances [22],

$$\overline{y^2} = \bar{y}^2 + \sigma_y^2. \tag{7}$$

Equation (7) can be interpreted as the power of a signal in the evaluated time interval T being composed of an average signal power and a signal power associated to fluctuations. In the case of cap testing, after the removal of drift effects, an appropriate offset shift sets the mean value of the signal to zero. Thus, the variance of the signal is equal to the signal power. The variance describes the dispersion of the disturbed signal. By definition, the output signal of a capped sensor contains only signal information due to disturbance effects violating the measurement process. Therefore, the standard deviation is interpreted as a standard uncertainty u_y due to signal distortion [23,24].

The mathematical description of noise characteristics and the definition of terminology, which are used in the following sections, are based on Buttkeus [25].

2.5. EMI Testing Device

The novel testing device targets the in-situ testing of capacitive displacement sensors in machine tool environments. It reproduces potential electrical settings of the spindle measurement setup.

The basis of the testing device is an electrically isolating polycarbonate frame, which is mounted on the machine tool table with ceramic elements in between (Figure 7). On top of the frame, a split shaft grounding ring is mounted. The two ring segments are placed on different heights, in order to prohibit a direct contact of fibers of the two different grounding shaft segments. The split shaft grounding ring electrically contacts a rotating test mandrel.

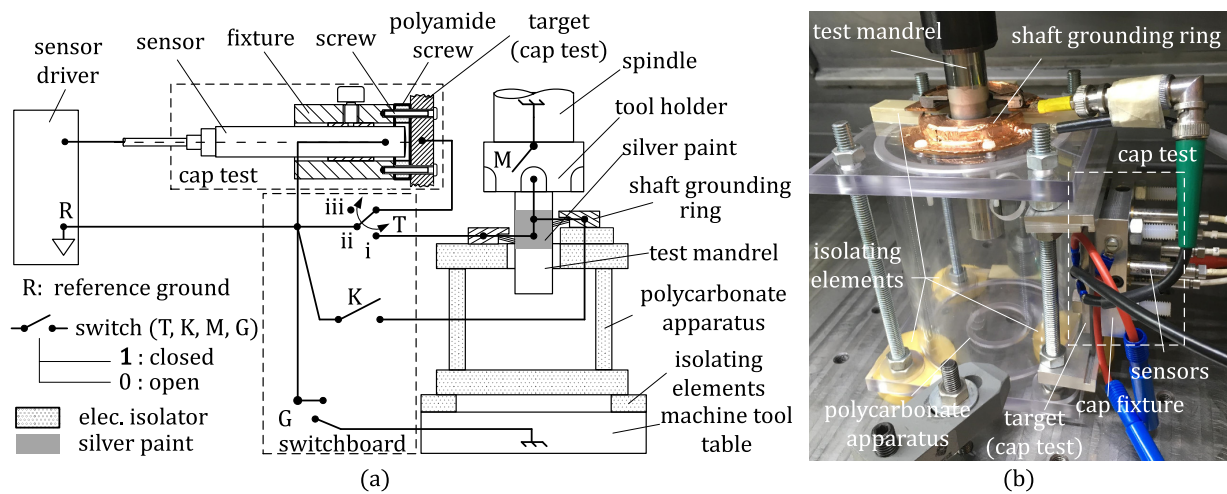


Figure 7. EMI testing device: (a) schematic; and (b) experimental setup on machine tool.

A metallic jig holds five capacitive displacement sensors. A brass collet in combination with a steel set screw fix the axial position of each sensor. The sensor housings are earthed on the reference ground of the measurement device. Thus, the sensor fixture and the sensor housing have the same potential. The sensors measure against a flat steel target. Target and sensor fixture are separated by a polycarbonate spacer. Four polyamide screws hold the fixture, spacer and target in place. This setup enables the galvanic separation of the sensor housing and the reference ground from the target.

The influence of the interface between spindle rotor and test mandrel is tested via two types of test mandrels: First, a standard steel test mandrel for geometric spindle testing establishes an electrical conducting interface to the spindle. Second, an electrically isolating cylinder, made of cotton fabric-base laminate with a phenolic resin matrix (EN PF CC 201, resofil) establishes a galvanic separation at the spindle interface. Both the conducting and isolating test mandrels are coated with conducting silver paint on the running surface for the fibers. Thus, an electrically conducting connection between the ring segments of the shaft grounding ring via the silver paint area on the test mandrels is ensured. In the case of the utilized cylindrical steel test mandrel (diameter 20 mm, length 160 mm), the mass ratio of silver paint to test mandrel was estimated to be below 1:100. Hence, the disturbing influence of the silver paint on the static loading of the tested spindle was negligible. If target and silver coating are balanced together, disturbing dynamic effects are minimized.

The different components of the testing device are wired to a switchboard-like device. This enables a convenient and fast switching between different electrical configurations. The switches $T-\{i, ii, iii\}$ and K allow the state simulation of a floating ground, a direct coupling to the reference ground R or a grounding path via a rotating test mandrel. The switching of M is accomplished by the exchange of the steel test mandrel with the resofil cylinder. The switch G in combination with switch M enables the electrical interconnection of machine tool interfaces with the reference ground R .

2.6. EMI Testing Procedure

The testing procedure aims at a quantitative characterization of the capacitive displacement sensor behavior in machine tool environments and is based on three sub-processes. Figure 8 shows the procedure in detail. The EMI testing device was utilized in corresponding experiments.

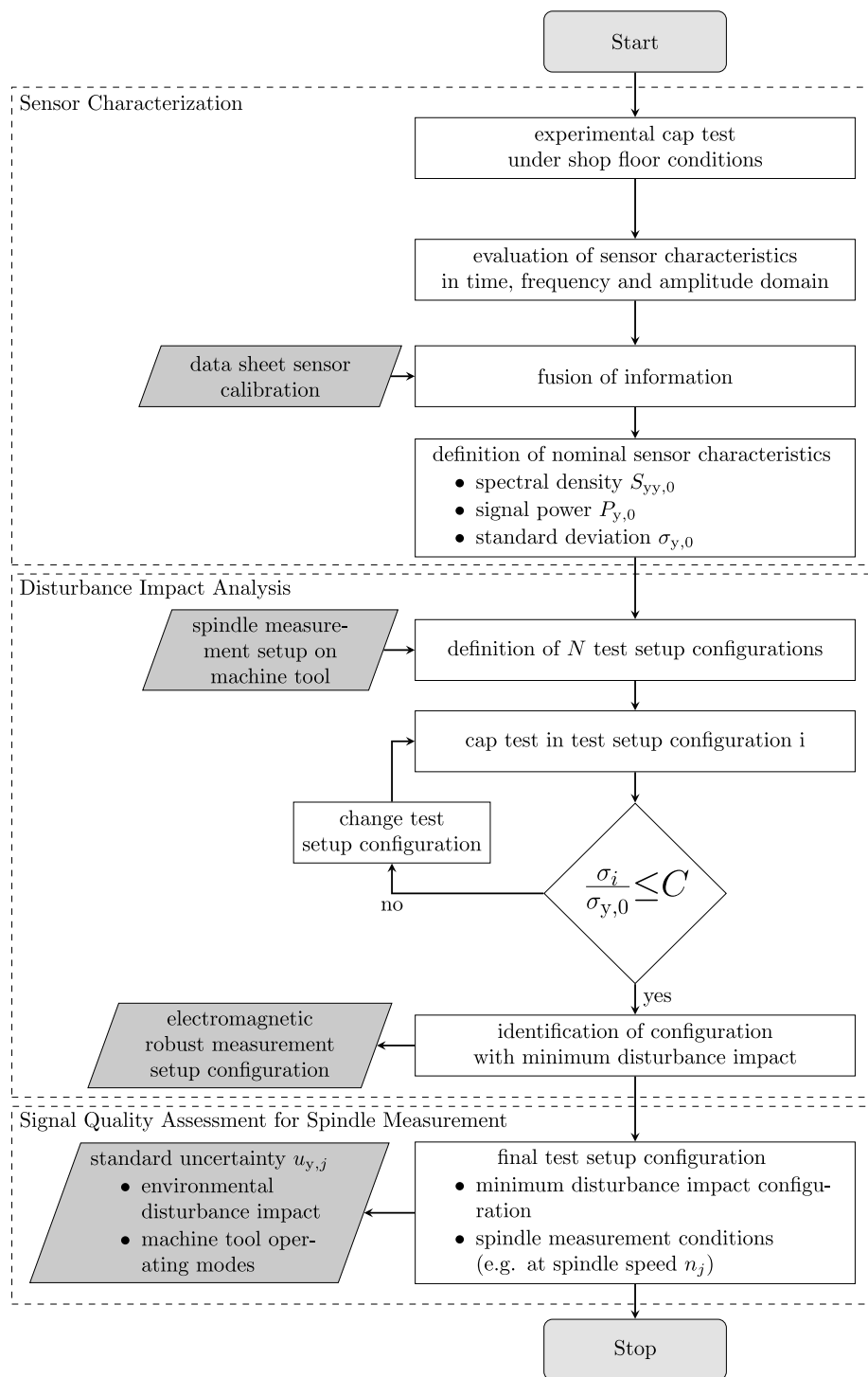


Figure 8. Flow chart of EMI testing procedure.

In the first sub-process, the sensor is characterized under shop floor conditions. The output signal is analyzed in frequency, time and amplitude domain. The shape of the spectral density function $S_{yy,0}$ characterizes the sensor behavior under these conditions. Further, specific frequency contents might appear, which are inherent characteristics of the tested sensor. For a quantification of the sensor signal characteristic,

the signal power $P_{y,0}$ and the standard deviation $\sigma_{y,0}$ are determined. Additionally, the available data of the manufacturer sensor calibration are incorporated and fused with the experimental data. Thus, a finger print of each individual displacement sensor under nominally undisturbed environmental conditions is created.

In the second sub-process, the specific spindle measurement setup for the intended test has to be defined. Based on this definition, interfaces between measurement setup and machine tool can be identified. The located interfaces determine the kind and number of electrical configurations of the EMI testing device.

Each testing device configuration is experimentally tested under appropriate machine tool operating modes. The evaluated standard deviations $\sigma_{y,i}$ are set in relation to the standard deviation $\sigma_{y,0}$ under benchmark environmental conditions. Based on information on the targeted measurement uncertainty, which has to be achieved, a threshold value C is defined. This value limits the acceptable ratio of $\sigma_{y,i}/\sigma_{y,0}$. This sub-sequence enables the identification of the electrical spindle measurement setup configuration with least achievable disturbance impact. Further, the effectiveness of appropriate attenuating mechanisms can be tested and verified.

In the third sub-process, after having identified a potential optimum electrical connection configuration, the behavior of the capped sensors under different machine tool operating modes is evaluated. These operating conditions are defined by the status of the numerical control (NC). Additionally, the influence of the rotating spindle at different speeds n_j needs to be analyzed. The following definitions of machine tool operating conditions are used:

- The measurement device behavior under shop floor conditions is tested on a currentless machine tool. This status is defined as *MT OFF*.
- The status *NC OFF* is defined by the circumstance that the machine tool is powered, but position control is not active.
- The activation of the position control of axes and drives to force the axes to maintain their current position is defined by *NC ON*. Depending on the type of control, either individual axes or the entire axis system is set in mode *NC ON*.
- The geometric testing of spindles is carried out under operational speeds n_i and the position control of the linear axis is set active. These operating modes are described by the term *SPEED*.

The sensors are tested under the defined operating modes and the standard deviations of the output signals are evaluated. The speed-dependent standard deviations $\sigma_{y,j}(n_j)$ are interpreted as standard uncertainties $u_{y,j}(n_j)$. They reflect disturbing influences due to environmental influence and noise for individual operating points during the geometric spindle measurement.

Depending on the prior knowledge of the disturbing influence of a specific machine tool on the measurement device, the procedure can be adapted. For instance, if the measurement device was already tested and characterized and from experience a reasonable electromagnetic compatible spindle measurement setup had already been found, only conducting the assessment of the signal quality for the upcoming spindle measurement would be necessary.

3. Results

In the beginning of this section, the inherent characteristics of a sensor are discussed. Afterwards, the sensor characteristics under disturbing environments are evaluated. Subsequently, the effects of the experimentally applied attenuation method are presented. Finally, the effectiveness of the proposed attenuation method is verified in different machine tool environments and in repeated tests. The switching configurations, which are discussed in the following, are indicated in Table 3.

Table 3. Exemplary testing device configurations according to Figure 7a.

No	Test Case	Switchboard Configuration						Description
		T			G	K	M	
		i	ii	iii				
1	V1	0	1	0	1	0	0	target coupled to machine tool table
2	D1	0	1	0	0	0	0	fully decoupled cap test
3	D2	1	0	0	0	1	1	target coupled to spindle
4	D3	1	0	0	0	1	0	decoupled spindle measurement setup
5	D4	0	1	0	1	0	0	target coupled to machine tool table

3.1. Sensor Characterization

The testing device was installed on the powerless Machine Tool A in Configuration D1 (Table 3). The observed sensor behavior under shop floor conditions represents mainly its inherent characteristics. Hence, this experimental case was defined as the benchmark case. Figure 9a shows the spectral density $S_{yy} =: S_{yy,0}$ for the frequencies $f \in [0 \text{ kHz}, 60 \text{ kHz}]$. The power of the signal over the whole frequency range is $P_y =: P_{y,0} = 59.5 \text{ nm}^2$ ($\sigma_y =: \sigma_{y,0} = 7.7 \text{ nm}$). The shape of the spectral density can be decomposed into five major effects. The noise floor, the red noise at low frequencies, wide and narrow band coloured noise accumulate almost 90% of the total signal power. The remaining power is accounted to narrowband noise lines. The probability density function of the signal $y(t)$ is symmetric (Figure 9b). The distribution is shaped like a normal distribution and has a kurtosis of 3.

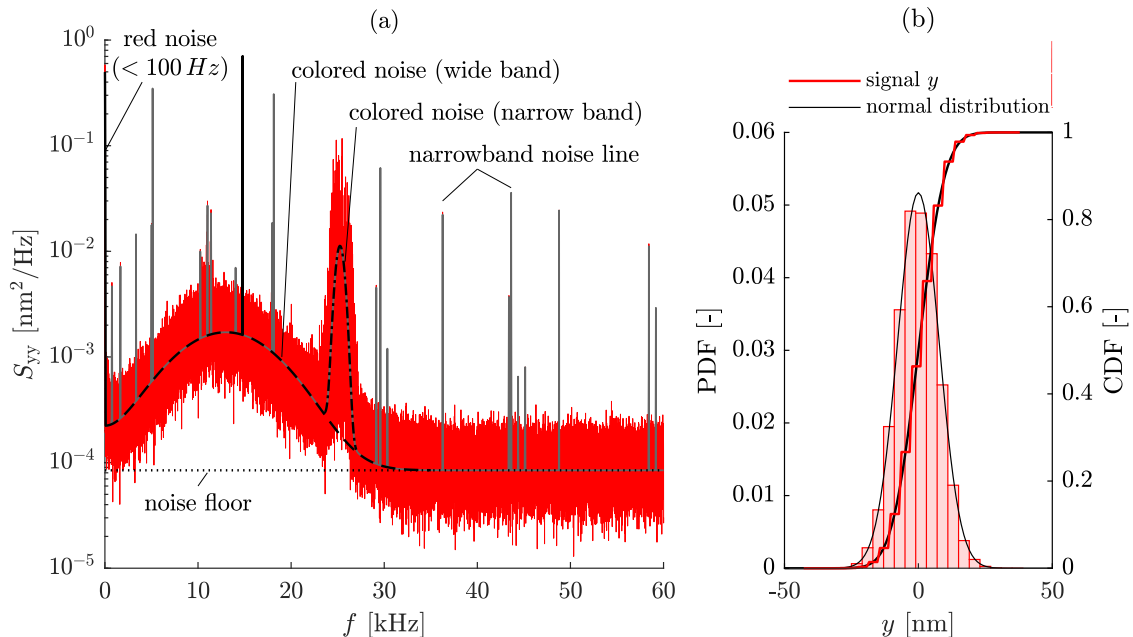


Figure 9. Cap test under shop floor conditions (MT OFF): (a) spectral density $S_{yy} (=: S_{yy,0})$ of output signal $y(t)$ with qualitative indication of noise effects; and (b) histogram and cumulative distribution function of signal $y(t)$ and for normally distributed values with $\mathcal{N}(\bar{y}, \sigma_y^2)$ for comparison.

Machine Tool A was next powered and set into Operating Mode NC ON. The testing device switching Configuration D2 was applied, which means that the target was electrically coupled to the spindle rotor. Figure 10 shows the results of the benchmark Case D1 in comparison to Case D2. The time records as well as the spectral densities show clear differences, regarding signal amplitudes, frequency content and signal

power. The disturbing influence of the spindle increases the output signal power by the factor of 300 in Case D2 compared to the benchmark Case D1. The electrical coupling of the spindle to the target leads to a marked increase in the spectral density for frequencies up to 35 kHz. Additionally, frequency lines at a fundamental frequency $f_f = 4$ kHz and corresponding harmonic frequencies $f_{h,i}$ with surrounding noise are visible. The distribution of the signal becomes positive skew (skewness of 0.8) and leptokurtic (kurtosis of 3.7), which is the result of an increased occurrence of peaks.

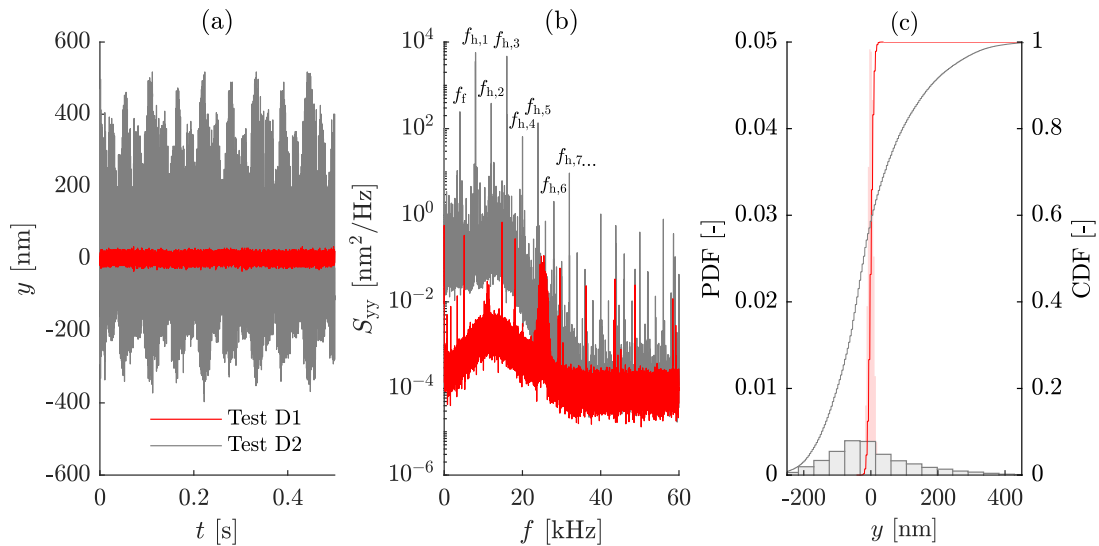


Figure 10. Comparison of cap tests in test device Configurations D1 (benchmark, fully decoupled cap test) and D2 (target coupled to spindle): (a) time domain; (b) spectral density; and (c) probability density and cumulative distribution function.

3.2. Electromagnetic Disturbance Impact Analysis

The experiments discussed in the following sections were carried out on Machine Tool A. The machine was fully powered. Configurations V1, D2, D3 and D4, indicated in Table 3, were tested. The sampling frequency was $f_s = 250$ kHz. The signal $y(t)$ was evaluated in terms of the RMS value y_{rms} , the mean value \bar{y} and the standard deviation σ_y . Throughout this section, the results of the same sensor are presented. The following sequence of machine tool operating modes was applied and each sub-sequence was held for $T = 9$ s:

1. The machine tool was turned ON, but position control was switched OFF (Operating Mode NC OFF).
2. The position control for spindle unit and linear axes were switched ON (Operating Mode NC ON).
3. The disturbance influence at different spindle speeds, in the range of 100 rpm–24,000 rpm, was tested (Operating Mode SPEED).
4. After the spindle had run down and stopped completely, the position control remained active (Operating Mode NC ON).
5. Finally, the position control was turned off (Operating Mode NC OFF). Thus, nominally, the same status as at the beginning of the test sequence was reached.

The results of the tests in Configurations *D2* and *D3* are depicted in Figure 11.

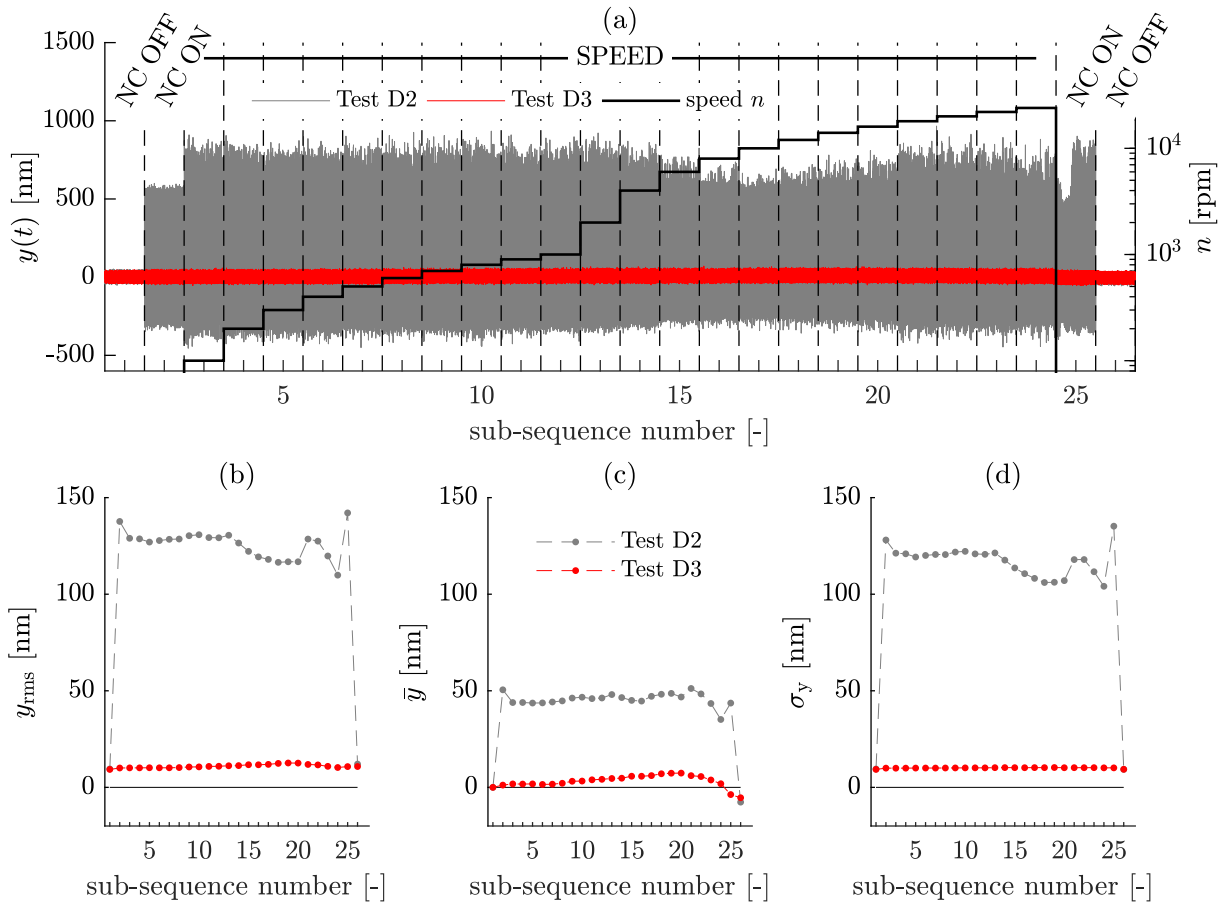


Figure 11. Comparison of electrical configurations with target coupled to spindle (Test *D2*) and electrically decoupled spindle measurement setup (Test *D3*): (a) signal $y(t)$ in time domain (sub-sequence: time duration $T = 9$ s and sampling frequency $f_s = 250$ kHz); (b) root-mean-square value y_{rms} ; (c) mean value \bar{y} ; and (d) standard deviation σ_y .

In Case *D2* and Operating Mode *NC OFF*, the signal standard deviation amounts to 9.5 nm. Switching to *NC ON* results in a significant increase of the signal amplitude. During the spindle speed testing, the signal standard deviation remains between 105 nm and 135 nm. Switching back to *NC OFF* leads to a decrease of signal amplitudes and to comparable standard deviations as in the beginning of the experiment. The changes of the mean value are in the range of $\Delta\bar{y} = 60$ nm.

In Configuration *D3*, the cap test is integrated into the electrical system of the machine tool, but electrically isolated at all machine tool interfaces. This configuration represents the attenuation proposal of Section 1.4.3 by galvanic separation at the spindle interface.

The recorded signal in each sub-sequence is symmetric with respect to the corresponding mean value. The range of changes in the mean value is bounded to $\Delta\bar{y} = 12.7$ nm. The signal standard deviation stays below $\sigma_y < 10.3$ nm over all operating conditions.

In test Configurations *V1* and *D4*, the target was electrically conductively coupled to the machine tool table. In Test *D4*, the indicated displacement was evaluated, whereas, in Test *V1*, the voltage U between machine tool table and reference ground was determined.

The recorded data of the sub-sequences under machine tool Operating Modes *NC ON* and *SPEED* were evaluated in frequency domain. The resulting data were graphically presented as a frequency map with the frequency f on the abscissa, the spindle speeds n on the ordinate and the magnitudes of the color-coded frequency components $|U(f)|$ and $|Y(f)|$ (Figure 12).

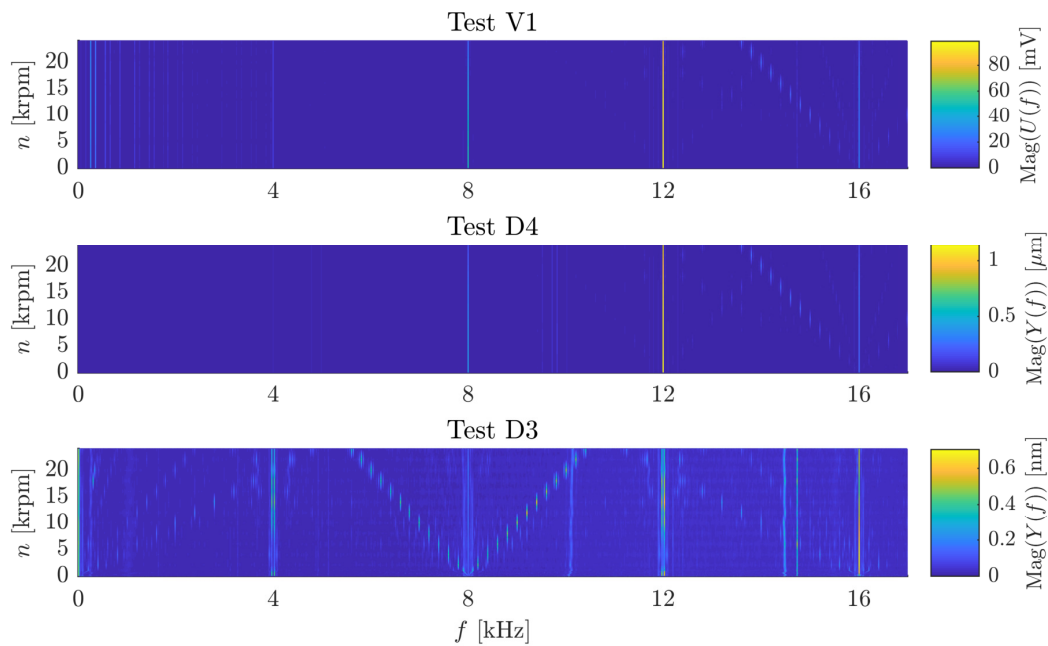


Figure 12. Frequency map: Test *V1*, voltage measurement in configuration target coupled to machine tool table; Test *D4*, displacement measurement in configuration target coupled to machine tool table; and Test *D3*, displacement measurement in configuration measurement device galvanically separated from machine tool.

Comparing the frequency maps for Tests *V1* and *D4*, three vertical distinguished lines are clearly visible at the frequencies 8 kHz, 12 kHz and 16 kHz. The galvanic separation of the measurement setup in Configuration *D3* results in a marked reduction of amplitudes. Comparing the scales of the frequency maps for Test *D4* in micrometers and for Test *D3* in nanometers, the maximum amplitude occurring in Case *D3* is approximately three orders of magnitude smaller than in Case *D4*.

3.3. Performance Testing of Attenuation Approach

The results of the experimental application of the proposed attenuation approach in Section 1.4.3 are presented in the following paragraphs. These experiments were considered to verify the performance of the proposed approach.

3.3.1. Performance Evaluation in Different Machine Tool Environments

The sensor behavior was evaluated in two different machine tool environments. The influence of a conducting spindle interface (Configuration *D2*) was compared to the behavior of a galvanically separated measurement device (Configuration *D3*). Typical output signals $y(t)$ of experiments on Machine Tools A and B in Operating Modes *NC OFF* and *NC ON* are shown in Figure 13.

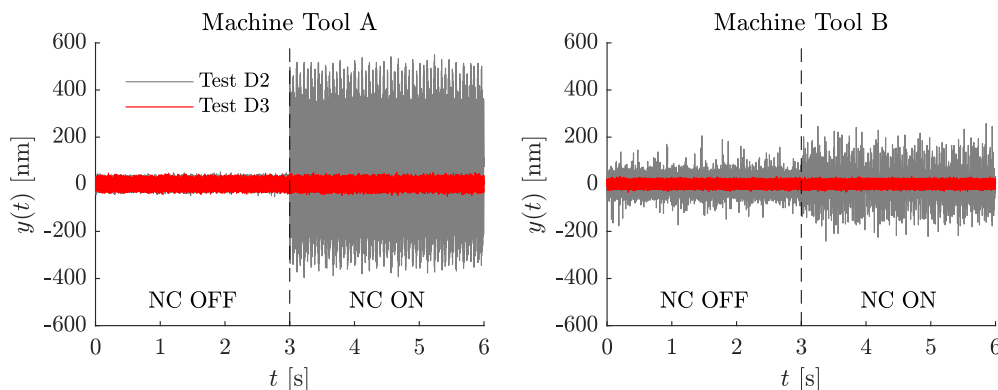


Figure 13. Output signal $y(t)$ for Configurations D2 (target coupled to spindle) and D3 (decoupled spindle measurement setup) in different machine tool environments and operating modes.

It is noticeable that the disturbance impacts on the measurement device differ in the environments of Machine Tools A and B in the case of the electromagnetically disturbed measurement setup. However, the signal characteristics of the output signal $y(t)$ in both machine tool environments are dependent on the state of the numerical control. On the contrary, in the case of the galvanically separated measurement setup, the signal characteristics are hardly affected by the choice of operating conditions.

Figure 14 shows the corresponding standard deviations and peak-to-peak values.

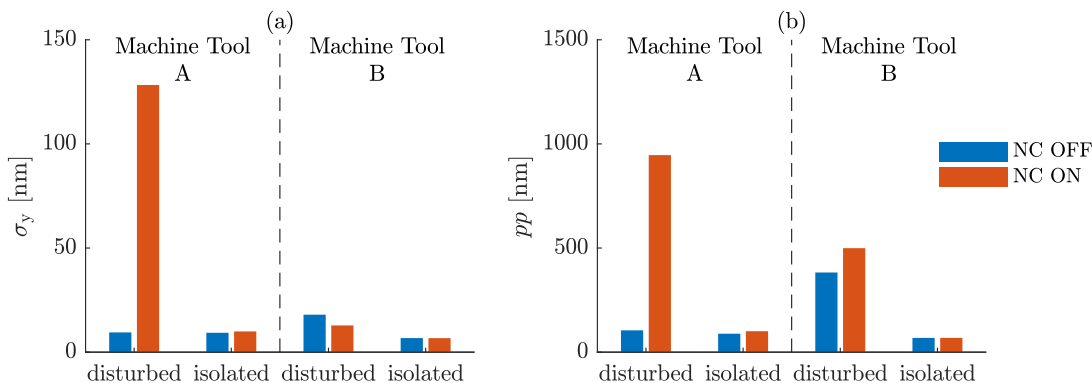


Figure 14. Evaluated parameters, standard deviation σ_y (a) and peak-to-peak value pp (b), of output signal $y(t)$ in testing device Configurations D2 (target coupled to spindle/“disturbed”) and D3 (decoupled spindle measurement setup/“isolated”) in different machine tool environments and under different operating modes.

In the environment of Machine Tool A the attenuation of the conductive coupling mechanism reduces the signal standard deviation and peak-to-peak values markedly. Particularly, these reductions are visible for the sensor behavior under machine tool Operating Mode NC ON. The standard deviation stays below 10 nm and the peak-to-peak value below 100 nm.

In the case of Machine Tool B, the signal power of the disturbed signal is comparatively small. Interestingly, switching from machine tool Operating Mode NC OFF to NC ON slightly decreases the signal standard deviation. On the contrary, the peak-to-peak value increases.

Nevertheless, applying the attenuation approach, namely the galvanic separation, results in a limitation of signal standard deviation, $\sigma_y < 6.8$ nm, and peak-to-peak values, $pp < 69$ nm. Especially, in the case of the peak-to-peak value, the achieved reductions in both machine tool environments are significant.

3.3.2. Repeatability of Attenuation Approach

The galvanically decoupled spindle measurement setup (Configuration D3) is repeatedly tested on Machine Tool A applying the previously described test sequence.

For each machine tool operating condition j and each measurement run i , the standard deviation $\sigma_{y,ij}$ was evaluated. The mean standard deviation $\bar{\sigma}_{y,j}$ corresponding to the j th operating condition was then determined. Figure 15 depicts the corresponding results. The estimated measurement uncertainty $U(k = 2)$ includes contributors due to the resolution of the analog-to-digital converter ($u_{LSB} \approx 1 \text{ nm}$) and variation in standard deviations $s_{\sigma_{y,ij}}$. An upper limit for the signal standard deviation of $\bar{\sigma}_{y,max}(k = 2) = 10.5 \text{ nm} \pm 2.2 \text{ nm}$, considering all machine tool operating modes, was identified.

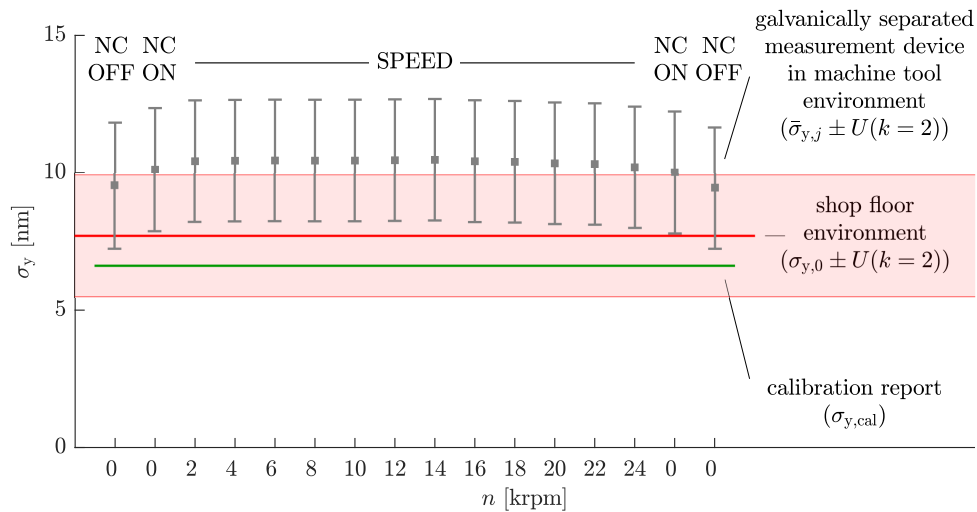


Figure 15. Repeatability test of galvanically separated measurement device tested in the environments of Machine Tool A and under different machine tool operating modes.

Compared to the standard deviation $\sigma_{y,0}(k = 2) = 7.7 \text{ nm} \pm 2.2 \text{ nm}$ of the benchmark Case D1, the signal standard deviation achieved in Configuration D3 is slightly higher, but comparable. Additionally, the measurement device shows a comparable performance in Configuration D3 as determined under laboratory calibration conditions by the manufacturer.

4. Discussion

The mechanical structure, axes, spindles, rotary axes and power electronics of a machine tool build an electrical network. The structural and electrical components are earthed on the safety ground. Electrical drives and controls may introduce disturbance voltages. In capacitive spindle measurements, the target, which is connected to the reference ground of the measurement device, and the capacitive transducer form a measuring circuit. Hence, the measurement system also constitutes an electrical network. Both networks, measurement system and machine tool, interact, which results in disturbed measurements.

The output signal of a disturbed sensor is distorted and noisy. Further, shifts in the mean value of such a signal are detectable. The impact of electromagnetic disturbances is superposed to the detected mechanical displacement of the target and might be erroneously interpreted as a mechanical displacement. Due to the electromagnetic origin of the signal disturbance, it can be interpreted as a pseudo motion.

In the previous section, describing experiments on Machine Tool A, the experimental detection of disturbing voltages between machine tool table and the reference ground of the measurement device

is presented. The disturbed output signal contains components with frequencies of 8 kHz, 12 kHz and 16 kHz. These are suspected to be harmonics of the fundamental frequency of 4 kHz, which corresponds to the pulse frequency of the axis drives. The voltage signal is strongly correlated with the disturbances occurring in displacement signals of the tested capped sensors. The ratio of magnitudes of voltage and displacement signal at the harmonic frequencies corresponds approximately to the sensitivity of the capacitive sensor. The implementation of electrically isolating elements and thus the galvanic separation of measuring circuit and machine tool results in significant attenuation of disturbances.

First, the results support the assumption that the machine tool acts as a disturbance source on capacitive measurements. Second, a non-negligible coupling mechanism between disturbing source and measurement device is conductive coupling. If the disturbances were only transferred by radiation, an isolator implemented at machine tool interfaces would have little impact on the transfer path and impact of disturbances. Nevertheless, the implemented isolator has to be chosen carefully, in order to keep the residual capacitive coupling below acceptable limits.

The tested capacitive measurement systems behaves differently in different machine tool environments. The measuring device may be highly prone or may respond rather robust to different machine tool environments. The proposed attenuation method, targeting electromagnetic disturbances coupling into the measurement system via conduction, enables a sensor performance, which is almost independent of the machine tool environment and machine tool operating conditions. The achieved repeatable sensor performance in machine tool environments and under different machine tool operating conditions is comparable to the calibrated and by the manufacturer specified performance.

Although the proposed disturbance attenuation method yields acceptable results, residual distortion is still present in the output signal of the tested capped sensors. Disturbance sources in the environment of the measurement device still may interact with the measurement system.

The remaining distortion effects potentially result from electromagnetic radiation, inductive and capacitive coupling effects. A valid option to reduce these coupling mechanisms is the reduction of the distributed characteristic of the measurement system. If the sensor, test mandrel and evaluation electronics were centralized in one shielded box, the mentioned coupling mechanisms could be further attenuated.

Other potential disturbances, which couple into the measurement system, may come from the power line of the measurement device or be generated in the power supply unit. These disturbance influences can be addressed by the utilization of line filters.

The shaft grounding ring, which ensures grounding of the rotating test mandrel, may also introduce disturbances or signal fluctuations. Insufficient contact pressure of fibers or varying contact pressure due to misalignment and radial throw of the test mandrel, may disturb the measurement signal. The electrical characteristics of the sliding contact are assumed to depend on spindle speed. In addition, the electrical properties of the sliding contact between fibers and test mandrel may change over time due to fiber and silver coating changes. The analysis of the assumed disturbing shaft grounding influences and a corresponding dynamic characterization has to be targeted in future work.

The proposed choice of the standard deviation as a quality parameter does not always adequately represent signal quality. The behavior of the capped sensor in the environment of Machine Tool B represents such a situation. Additionally, radio technology devices can generate temporary shifts of the signal offset. Insufficiencies in the grounding system of the spindle measurement setup, tend to generate asymmetric signals. The shape of the signal histogram is sensitive to these disturbance effects. Therefore, skewness and kurtosis are potential parameters to capture these effects. The additional use of these parameters together with the mean value and standard deviation seems promising and is also subject to future work.

The design of a novel electromagnetic compatible spindle measurement setup, which is based on the results of this study, is in process.

For the disturbance attenuation at the spindle interface, a test mandrel with a shaft made of silicon nitride Si_3N_4 is intended. This material is an electrical insulator. A steel precision sphere as target is attached to one end of the shaft in order to provide an appropriate measuring surface. On the one hand, this arrangement ensures a galvanic separation of the spherical target from the spindle. On the other hand, the small capacity of the shaft restricts capacitive coupling between measuring circuit and machine tool.

Silicon nitride offers electrical isolating properties, the necessary flexural strength and a low coefficient of thermal expansion (Table 4). Compared to steel, especially 440C, a material typically used for test mandrels, silicon nitride has a higher Young’s modulus and lower density. Thus, bending and deflection of the shaft due to dynamic effects and inertial forces are reduced. In comparison to, e.g., aluminium oxide, silicon nitride offers higher flexural strength and thus higher mechanical safety.

At the machine tool table interface, ceramic spacers with appropriate width are inserted, in order to provide an electrically non-conducting interface with low capacity.

Table 4. Physical properties of potential test mandrel materials.

Material		Stainless Steel	Silicon Nitride	Aluminium Oxide
Type		X105CrMo17 1.4125/440C [26]	Si_3N_4 CS45 [27]	Al_2O_3 CS20 [27]
Density ρ	[g/cm ³]	7.70	3.24	3.9
Yield Strength $R_{p,0.2}$	[MPa]	450	-	-
Flexural Strength σ at 20 °C	[MPa]	-	900	350
Weibull module m	[-]	-	25	12
Young’s module E	[GPa]	220	320	380
Poisson’s ratio ν	[-]	0.3	0.28	0.20
Thermal conductivity λ at 20 °C	[W/(m K)]	15	25	30
Thermal expansion coefficient α_{th} for 20–100 °C	[10 ⁻⁶ /K]	10.4	2	6.5
Electrical resistivity ρ_{el} at 20 °C	[cm]	$\approx 10^{-6}$	$\approx 10^{12}$	$\approx 10^{14}$
Permittivity ϵ at 1 MHz	[-]	-	7	10

5. Conclusions

Electromagnetically induced disturbances can extensively corrupt capacitive machine tool spindle measurements. Responsible for such disturbances are electrical controls and power electronics of the machine tool. The resulting signal distortion leads to reduced signal-to-noise ratios and increased measurement uncertainties. Electromagnetic radiation is generally suspected as the transmitting mechanism for disturbances. However, it is shown in this paper that disturbances also couple into the measurement system via electrical conduction.

Electrical isolators offer an effective attenuation of this coupling mechanism without violating the signal. The isolators decouple the measuring circuit from the machine tool circuit. To suppress the remaining capacitive coupling, the isolator capacities shall be much smaller than the capacity of the measuring circuit. The results of the validation experiments show that the impact of machine tool disturbances can be reduced significantly. Signal power, peak-to-peak values and the spectral density of the sensor output signal, which were recorded under machine tool operating, modes are comparable to the sensor performance achieved under laboratory calibration conditions. The robustness of the attenuation method was verified in different machine tool environments.

The proposed EMI testing device targeting at electromagnetic interference enables the in-situ testing of displacement sensors in machine tool environments. The presented methods for signal quality assessment as well as the developed EMI testing procedure allow a quick evaluation of sensor performance in machine

tool environments. Finally, the information gathered during the testing procedure can be directly used for the measurement uncertainty budget of the spindle measurement on the corresponding machine tool.

Author Contributions: Conceptualization, S.B.; Data curation, S.B.; Formal analysis, S.B.; Funding acquisition, S.W. and K.W.; Investigation, S.B.; Methodology, S.B.; Resources, K.W.; Software, S.B.; Validation, S.B.; Visualization, S.B.; Writing—original draft, S.B.; and Writing—review and editing, S.W. and K.W.

Funding: This research received no external funding.

Acknowledgments: The authors thank particularly Wolfgang Knapp and Karl Ruhm for fruitful discussions, contribution of ideas, patient guiding and the critical review of the manuscript. Thanks are also given to Andreas Kunz, who shared his knowledge of electronics. The authors also thank the reviewers, who helped to improve the manuscript with their comments.

Conflicts of Interest: The authors declare no conflict of interest.

Abbreviations

The following abbreviations are used in this manuscript:

CDF	Cumulative Density Function
EMC	Electromagnetic Compatibility
EMI	Electromagnetic Interference
ENOB	Effective Number of Bits
ETH	Swiss Federal Institute of Technology
IWF	Institute of Machine Tools and Manufacturing
MT	Machine Tool
NC	Numerical Control
PDF	Probability Density Function
PP	Peak-to-Peak
PWM	Pulse Width Modulation
RMS	Root-Mean-Square
SCR	Silicon Controlled Rectifier
SGR	Shaft Grounding Ring
SINAD	Signal-to-Interference ratio including Noise And Distortion
SNR	Signal-to-Noise Ratio
UPR	Undulations Per Revolution

References

1. Tlustý, J. Systematik und Methodik der Prüfung von Werkzeugmaschinen. *Microtechnic* **1959**, *13*, 169–187.
2. Abele, E.; Altintas, Y.; Brecher, C. Machine tool spindle units. *CIRP Ann.-Manuf. Technol.* **2010**, *59*, 2, 781–802. [\[CrossRef\]](#)
3. Bryan, J.B.; Clouser, R.; Holland, E. Spindle Accuracy. *Am. Mach.* **1967**, *612*, 149–164.
4. *Test Code for Machine Tools—Part 7: Geometric Accuracy of Axes of Rotation*; ISO 230-7:2015; International Organization of Standardization: Geneva, Switzerland, 2015.
5. Marsh, E.R. 3.3 Capacitive Sensors. In *Precision Spindle Metrology*; DEStech Publications Inc.: Lancaster, PA, USA, 2008; pp. 44–58.
6. Rohrbach, C. D3. Kapazitive Geber. In *Handbuch für Elektrisches Messen Mechanischer Grössen*; VDI-Verlag: Düsseldorf, Germany, 1967; pp. 149–150.
7. Sheridan, T. Section 3—Grounding, Interference, and Electrical Noise. In *Know your Machine Tool*; Lion Precision: St. Paul, MN, USA, 1991; pp. 15–20.
8. Baxter, L.K. 12 Noise and stability. In *Capacitive Sensors*; Series on Electronics Technology; Anderson, J.B., Herrick, R.J., Eds.; IEEE Press: New York, NY, USA, 1997; pp. 197–213.

9. *Electromagnetic Compatibility (EMC)—Part 1–2: General—Methodology for the Achievement of Functional Safety of Electrical and Electronic Systems Including Equipment with Regard to Electromagnetic Phenomena*; IEC 61000-1-2:2016; International Electrotechnical Commission: Geneva, Switzerland, 2016.
10. Weidauer, J.; Messer, R. EMC and electrical drives. In *Electrical Drives—Principles, Planning, Applications, Solutions*; Publicis Publishing: Erlangen, Germany, 2014.
11. Schwab, A.J.; Kürner, W. *Elektromagnetische Verträglichkeit-6., Bearbeitete und Ergänzte Auflage*; Springer: Berlin/Heidelberg, Germany, 2011.
12. Siemens AG. 1.9.4 Bearing currents caused by steep voltage edges on the motor. In *SINAMICS—Low Voltage Engineering Manual, Version 6.5*; Siemens AG: Nuremberg, Germany, 2017.
13. Dresig, H.; Fidin, A. Parameterwerte von Maschinenelementen und Baugruppen. In *Schwingungen Mechanischer Antriebssysteme—Modellbildung, Berechnung, Analyse, Syntese*; Springer: Berlin/Heidelberg, Germany, 2014; pp. 195–240.
14. Böhl, S.; Weikert, S.; Wegener, K. Improving robustness of capacitive displacement measurements against electromagnetic disturbances in machine tool environments. *Lamdamap XIII* 2019, 1, 59–68.
15. Gutnikov, V.S.; Lenk, A.; Mende, U. Elektronische Meßwandler für kapazitive und induktive Aufnehmer. In *Sensorelektronik*; Trumpold, H., Woschni, E.G., Eds.; VEB Verlag Technik: Berlin, Germany, 1984; pp. 236–253.
16. Breitenbach, A. A method for determining the signal-to-noise ratio of sensors by spectral analysis. *IEEE Instrum. Meas. Technol. Conf.* 1997, 1, 457–462.
17. Drahm, W.; Schrüfer, E. Wieviele effektive Bit hat ein analoges Signal? *Tech. Mess.* 1994 12, 61, 492–495.
18. *Test Code for Machine Tools—Part 3: Determination of Thermal Effects*; ISO 230-3:2007; International Organization of Standardization: Geneva, Switzerland, 2007.
19. Böhl, S.; Knapp, W. Observer-based compensation of thermal disturbances for linear displacement sensors. *CIRP Ann.* 2019, 68, 543–546. [[CrossRef](#)]
20. Palme, F.; Schrüfer, E. Berechnung der Signalleistung im Zeit-und Frequenzbereich-eine Methode zur Charakterisierung von Sensoren. *Tech. Mess.* 1998, 65, 370–377. [[CrossRef](#)]
21. Profos, P. Mittel zur mathematischen Beschreibung stochastischer Signale. In *Einführung in die Systemdynamik*; Teubner: Stuttgart, Germany, 1982; pp. 39–51.
22. Böme, J.F. Modelle für gemessene Signale: Stochastische Signale. In *Stochastische Signale—Eine Einführung in Modelle, Systemtheorie und Statistik*; Teubner: Stuttgart, Germany, 1993; pp. 91–168.
23. *Evaluation of Measurement Data—Guide to the Expression of Uncertainty in Measurement*; JCGM 100: 2008; International Organization for Standardization (ISO): Geneva, Switzerland, 2008.
24. Weise, K.; Wöger, W. Meßunsicherheit. In *Meßunsicherheit und Messdatenauswertung*; Bortfeldt, J., Hauser, W., Rechenberg, H., Eds.; WILEY-VCH Verlag GmbH: Weinheim, Germany, 1999.
25. Buttkus, B. Characterization of Random Processes in the Time and Frequency Domains. In *Spectral Analysis and Filter Theory in Applied Geophysics*; Springer: Berlin/Heidelberg, Germany, 2000; pp. 152–178.
26. Martienssen, W.; Warlimont, H. Part 3—Classes of Materials—Martensitic and Martensitic-Ferritic Chromium Steels. In *Springer Handbook of Condensed Matter and Materials Data*; Springer: Berlin/Heidelberg, Germany, 2005; pp. 250–252.
27. Ceramdis GmbH. *Kennwerte keramischer Werkstoffe*; Ceramdis GmbH: Elsau, Switzerland, 2016. Available online: http://www.ceramdis.com/images/content/ceramdis_kennwerte_keramische_werkstoffe_de.pdf (accessed on 27 August 2019).

